Available online at www.sciencedirect.com
ScienceDirect
International Journal of Mass Spectrometry 266 (2007) 92–96
International Journal of Mass Spectrometry
www.elsevier.com/locate/ijms

Dissociative ionization of JP-10 ($C_{10}H_{16}$) by electron impact

C.Q. Jiao [a], C.A. DeJoseph Jr. [b], A. Garscadden [b,*]

[a] *Innovative Scientific Solutions Inc., Dayton, OH 45440-3638, USA*
[b] *Air Force Research Laboratory, Wright-Patterson AFB, OH 45433-7251, USA*

Received 28 June 2007; received in revised form 19 July 2007; accepted 19 July 2007
Available online 26 July 2007

Abstract

Ionization of JP-10 ($C_{10}H_{16}$, exo-tricycle [5.2.1.$0^{2,6}$] decane) by electron impact has been studied using Fourier transform mass spectrometry. Absolute total and partial ionization cross-sections have been measured as functions of the electron energy in the range of 10–200 eV. The major channel of parent ion fragmentation at low energies (<27 eV) produces $C_9H_{13}^+$, and at higher energies, $C_5H_7^+$. Possible fragmentation mechanisms are discussed.
Published by Elsevier B.V.

Keywords: JP-10; Fuel; Ionization; Electron impact; Fragmentation

1. Introduction

JP-10 is a synthetic fuel composed almost exclusively of the exo isomer of tricycle [5.2.1.$0^{2,6}$] decane, also called exo-tetrahydrodicyclopentadiene ($C_{10}H_{16}$). Due to its strained cyclic structure (Fig. 1), it has a high volumetric energy density, with a heat value of 39.6 MJ/L, substantially higher than the petroleum-based fuels such as JP-8, with heat value of 34.5 MJ/L, which makes it suitable for certain propellant applications including missiles, supersonic-combustion ramjets and pulse-detonation engines. One problem with JP-10 and other liquid hydrocarbon fuels is that their ignition and combustion kinetics are relatively slow. Although many combustion research studies [1–22] have been carried out on JP-10, its detailed combustion mechanisms still remain to be explored. Products of the thermal decomposition of JP-10 have been investigated. It is also important to understand the mechanisms of JP-10 fragmentation breakdown [16,19,20]. In one particular study it is proposed that one of the initial steps of JP-10 fragmentation is through the rupture of a C–H bond of a CH_2 group, and another step is through the bond cleavage between C1 and C6 atoms as labeled in Fig. 1 [16].

Plasma assisted ignition and combustion (PAI and PAC) have been of great interest in recent years. Literature in this area, especially using low temperature nonequilibrium plasmas, has been summarized in a recent, comprehensive review by Starikovskaia [23]. Different mechanisms including ion chemistries have been proposed and investigated, and models taking into account elementary process such as electron impact ionization have been developed [23]. The possibility offered by nonequilibrium plasmas to guide a parameter such as the mean electron energy provides researchers with an opportunity to change the energy branching in the plasma from mainly gas heating and excitation of low-energy vibrational modes to excitation of high-energy electronic states and ionization. In an experiment by Maly and Vogel, extremely high electric fields have been realized that lead to almost complete gas dissociation and ionization of CH_4–air mixtures [24]. Studies of nanosecond gas breakdown in long tubes, called “fast ionization wave”, which is promising for plasma applications due to efficient gas excitation and ionization by high electric fields, have been reviewed recently [25]. In summary, charged particles in plasmas are of high interest, and the manipulation of charged particle energies adds a new dimension to the area of PAI and PAC.

This paper reports our recent study of ion formation in JP-10 by electron impact. Absolute total and partial ionization cross-sections as functions of electron energy will be presented.

* Corresponding author at: Propulsion Directorate, Air Force Research Laboratory, AFRL/PR, Bldg. 18A, 1950 Fifth Street, Area B, Wright-Patterson AFB, OH 45433-7251, USA. Tel.: +1 937 255 2246; fax: +1 937 656 4657.
E-mail address: alan.garscadden@wpafb.af.mil (A. Garscadden).

1387-3806/$ – see front matter. Published by Elsevier B.V.
doi:10.1016/j.ijms.2007.07.012

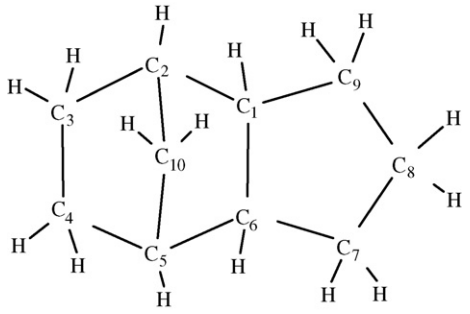

Fig. 1. Structure of JP-10.

Fragmentation mechanisms of the charged JP-10 molecule will be discussed.

2. Experimental

All of the experiments were performed using a modified Extrel Fourier transform mass spectrometry (FTMS) equipped with a cubic ion cyclotron resonance trapping cell (5 cm on a side) and a 2 T superconducting magnet [26]. The theory and methodology of FTMS have been well documented in the literature [27–29]. An experimental diagram is shown in Fig. 2. JP-10 was mixed with Ar (99.999%, Matheson) in a ratio of about 1:3 to a total pressure of ~4 Torr, as determined by capacitance manometer. The mixture was then admitted through a precision leak valve (Varian controlled leak valve) into the FTMS system. Ions are formed by electron impact in the trapping cell at pressures in the 10^{-7} Torr range. An electron gun (Kimball Physics ELG2, Wilton, NH) irradiates the cell with a few hundred picocoulombs of low-energy electrons, with the electron energy spread of about 0.25 eV plus the space charge well of the beam [30]. The motion of the ions in the cell is constrained radially by the superconducting magnetic field and axially by an electrostatic potential (trapping potential) applied to the trap faces that are perpendicular to the magnetic field. The trapping potential is usually set to 10 V. The trapping cell has been modified by adding a pair of screen electrodes in front of the trapping plates, which improves the trapping potential profile in the cell in a way that, with the screen electrodes grounded, the potential drop over most of the volume of the cell (between the two screen electrodes) is only ~0.3 V [31]. Combining the energy spread in the electron source and the potential drop in the trapping cell, we estimate the uncertainty of the ionizing electron energies in the FTMS trapping cell to be ±0.6 eV. Ions of all mass-to-charge ratios are excited simultaneously and coherently (that is, after excitation, there are only negligibly small phase differences among ions of the same mass-to-charge ratio) into cyclotron orbits using Stored Waveform Inverse Fourier Transform (SWIFT) [32] applied to two opposing trap faces which are parallel to the magnetic field. Following cyclotron excitation, the image currents induced on the two remaining faces of the trap are amplified, digitized and Fourier analyzed to yield a mass spectrum.

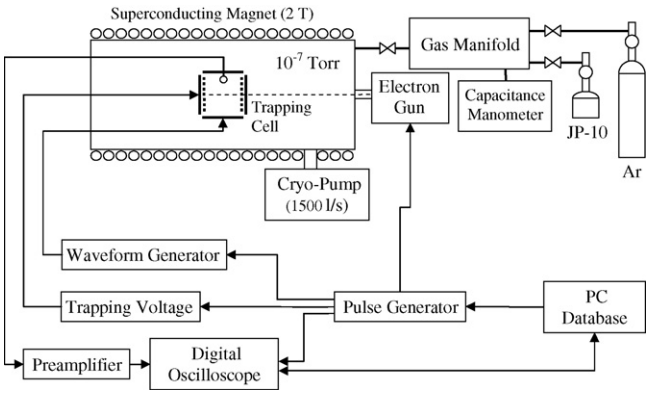

Fig. 2. Fourier-transfer mass spectrometry apparatus.

FTMS is an established technique for studying the kinetics of charged particle reactions, in which the ion peak heights are used to evaluate the number of ions in the cell [33]. In the study of the electron impact ionization cross-sections, the intensity ratios of the ions from JP-10 to Ar^+ give cross-sections relative to those for electron impact ionization of Ar [34], since the pressure ratio of JP-10 to Ar is known. The pressure ratio of JP-10 to Ar in the trapping cell region is equal to the pressure ratio in the manifold, based on the geometry of our FTMS instrument in which both in-flow and out-flow of the gas in the trapping cell region can be characterized as diffusive [31].

3. Results and discussion

Electron impact ionization of JP-10 is found to produce the parent ion and 36 fragment ions that have ionization cross-sections with peak values larger than 5×10^{-18} cm^2 in the electron energy range of 10–200 eV: $C_{10}H_{16}^+$, $C_9H_{13}^+$, $C_8H_{9,11,12}^+$, $C_7H_{7-12}^+$, $C_6H_{5-10}^+$, $C_5H_{3,5-9}^+$, $C_4H_{2-7}^+$, $C_3H_{1,6}^+$ and $C_2H_{3,5}^+$. The total cross-section and partial cross-sections of the 8 most important ions as functions of the electron energy are shown in Fig. 3. As an aid to plasma modelers, the experimental cross-section data were fitted to an empirical function:

$$\sigma(E) = c_1(1 - \exp(-c_2(E - c_3)^2)) \cdot \exp(-c_4(E - c_5)^2),$$

where σ is the cross-section and c_1–c_5 are the fitting parameters, among which c_1 is considered to scale the peak amplitude, c_3 is approximately the threshold energy and c_5 is approximately the peak energy, if $c_5 \gg c_3$. In the above, $\sigma(E) \equiv 0$ for $E < c_3$. The resultant set of coefficients from fitting the cross-section data for the 37 observed ions are shown in Table 1, and fitting curves for the 8 most important ions are included in Fig. 3. Please note that in Fig. 3 the fitting curve for the total cross-section is derived by summing the 37 analytic fits, in good agreement with the experimental data, suggesting the effectiveness of the above fitting function. The least-squares fits were performed on the data weighted by the statistical error, which was assigned a value of ±5% or 6×10^{-19} cm^2, whichever was larger. The estimated total error in the data, including the uncertainty in the reference cross-section for Ar and the error in the pressure measurement, is +18%. The two coefficients determined from the energy scale, c_3 and c_5, were corrected from the raw data to give $c_3(C_{10}H_{16}^+) = 9.35$ eV. This correction factor was −0.13 eV and

Table 1
Fitting parameters for electron impact ionization cross-sections

Ions	c_1 ($\times 10^{-16}$ cm^2)	c_2 ($\times 10^{-2}$ eV^{-2})	c_3 (eV)	c_4 ($\times 10^{-5}$ eV^{-2})	c_5 (eV)
$C_5H_7^+$	2.349 ± 0.038	0.56 ± 0.03	11.75 ± 0.11	5.5 ± 0.5	100.8 ± 1.9
$C_6H_7^+$	2.036 ± 0.034	0.65 ± 0.04	11.23 ± 0.14	7.8 ± 0.5	111.4 ± 1.2
$C_9H_{13}^+$	1.681 ± 0.026	2.07 ± 0.14	9.60 ± 0.10	5.3 ± 0.4	112.2 ± 1.6
$C_7H_{11}^+$	1.659 ± 0.026	1.66 ± 0.11	10.58 ± 0.10	5.2 ± 0.4	107.7 ± 1.6
$C_7H_{10}^+$	1.481 ± 0.023	1.72 ± 0.12	9.72 ± 0.10	4.2 ± 0.4	102.3 ± 1.9
$C_3H_3^+$	1.359 ± 0.471	0.06 ± 0.01	14.81 ± 0.31	2.0 ± 1.6	0.0 ± 119
$C_6H_8^+$	1.069 ± 0.017	1.42 ± 0.11	10.18 ± 0.14	5.0 ± 0.4	107.1 ± 1.6
$C_6H_5^+$	0.888 ± 0.016	0.36 ± 0.04	15.13 ± 0.33	10.1 ± 0.6	112.2 ± 1.1
$C_3H_5^+$	0.908 ± 0.089	0.21 ± 0.02	16.03 ± 0.22	1.5 ± 0.7	0.0 ± 57
$C_7H_9^+$	0.849 ± 0.014	1.84 ± 0.17	11.66 ± 0.19	7.5 ± 0.4	118.3 ± 1.3
$C_5H_6^+$	0.828 ± 0.013	0.98 ± 0.08	9.92 ± 0.19	5.3 ± 0.4	108.5 ± 1.6
$C_7H_7^+$	0.686 ± 0.012	0.48 ± 0.05	13.45 ± 0.34	9.0 ± 0.5	114.6 ± 1.1
$C_{10}H_{16}^+$	0.668 ± 0.010	2.23 ± 0.19	9.35 ± 0.15	3.2 ± 0.3	111.2 ± 2.6
$C_5H_5^+$	0.586 ± 0.011	0.42 ± 0.05	16.62 ± 0.39	9.0 ± 0.6	111.6 ± 1.2
$C_5H_8^+$	0.572 ± 0.009	0.88 ± 0.07	10.01 ± 0.21	3.5 ± 0.4	99.6 ± 2.6
$C_8H_{11}^+$	0.528 ± 0.008	2.28 ± 0.23	10.59 ± 0.20	4.6 ± 0.4	115.2 ± 1.9
$C_4H_3^+$	0.499 ± 0.318	0.04 ± 0.02	16.71 ± 0.79	2.7 ± 2.6	0.0 ± 153
$C_4H_5^+$	0.333 ± 0.006	0.30 ± 0.04	16.58 ± 0.51	6.3 ± 0.6	102.2 ± 2.7
$C_8H_{12}^+$	0.332 ± 0.005	2.34 ± 0.27	10.41 ± 0.26	3.8 ± 0.4	112.5 ± 2.2
$C_6H_6^+$	0.276 ± 0.005	0.30 ± 0.04	10.01 ± 0.81	8.8 ± 0.6	114.5 ± 1.2
$C_6H_9^+$	0.237 ± 0.004	1.50 ± 0.22	11.48 ± 0.44	5.5 ± 0.4	117.9 ± 1.8
$C_4H_2^+$	0.272 ± 0.147	0.03 ± 0.02	19.73 ± 1.80	5.3 ± 4.3	54.1 ± 91.9
$C_4H_7^+$	0.174 ± 0.003	0.70 ± 0.10	16.02 ± 0.62	5.2 ± 0.5	102.7 ± 2.1
$C_2H_3^+$	0.174 ± 0.056	0.08 ± 0.02	21.52 ± 1.19	1.0 ± 1.5	0.0 ± 228
$C_3H_2^+$	0.183 ± 0.092	0.08 ± 0.02	29.49 ± 1.30	2.1 ± 2.3	0.0 ± 161
$C_7H_{12}^+$	0.132 ± 0.002	2.33 ± 0.53	11.96 ± 0.60	4.1 ± 0.4	118.9 ± 2.7
$C_5H_3^+$	0.140 ± 0.030	0.05 ± 0.02	24.31 ± 1.86	5.8 ± 3.6	73.8 ± 50.5
$C_4H_6^+$	0.118 ± 0.002	0.51 ± 0.10	13.94 ± 0.92	4.0 ± 0.6	103.8 ± 3.4
$C_4H_4^+$	0.122 ± 0.002	0.14 ± 0.03	19.11 ± 1.53	6.8 ± 1.3	94.0 ± 7.3
$C_6H_{10}^+$	0.098 ± 0.002	2.11 ± 0.58	12.26 ± 0.75	3.3 ± 0.5	116.4 ± 4.0
C_3H^+	0.141 ± 0.136	0.07 ± 0.03	31.59 ± 1.87	3.1 ± 4.4	0.0 ± 213
$C_3H_4^+$	0.089 ± 0.002	0.69 ± 0.29	9.47 ± 2.03	6.6 ± 0.8	136.2 ± 3.7
$C_2H_5^+$	0.070 ± 0.029	0.08 ± 0.03	9.22 ± 2.29	0.8 ± 2.3	0.0 ± 400
$C_5H_9^+$	0.069 ± 0.002	0.83 ± 0.26	12.23 ± 1.27	3.2 ± 0.9	105.4 ± 5.8
$C_7H_8^+$	0.071 ± 0.002	1.23 ± 0.64	18.07 ± 1.85	8.7 ± 1.1	115.5 ± 2.8
$C_3H_6^+$	0.064 ± 0.030	0.14 ± 0.06	22.44 ± 2.60	1.8 ± 2.8	0.0 ± 212
$C_8H_9^+$	0.048 ± 0.002	2.21 ± 2.03	21.82 ± 2.43	9.5 ± 1.6	114.4 ± 3.8

The 37 ions are listed in order of decreasing importance. Also included are their standard deviations derived from the least-squares fit to the measured data. In some cases, the fitted values for c_5 converged to 0 but were statistically insignificant.

the raw data shown in Fig. 3 was likewise corrected by this amount. As seen in Fig. 3, the total ionization cross-section reaches a maximum of 2.19×10^{-15} cm^2 at 110 eV. The parent ion $C_{10}H_{16}^+$ is significant throughout the energy range studied. The most abundant fragment ion from threshold to 27 eV is $C_9H_{13}^+$. Above 27 eV, $C_5H_7^+$ becomes dominant. Other important fragment ions include $C_7H_{10}^+$, $C_7H_{11}^+$, $C_6H_8^+$, and $C_6H_7^+$.

The product ion population from JP-10 is dramatically different than those from non-cyclic alkanes, such as *n*-octane whose ionization cross-section has been studied by our group previously [35], in two aspects: (1) for non-cyclic alkanes, even-electron ions are considerably more abundant than the odd-electron ions, i.e., $C_nH_{2n+1}^+$ intensity > $C_nH_{2n}^+$ intensity [35]; while for JP-10, certain odd-electron ions are rather pronounced, such as $C_7H_{10}^{\bullet+}$, which are radical ions and thus are more chemically active. (2) The M-15 ion, i.e., formed by loss of CH_3 from the parent ion, is absent for large non-cyclic alkanes such as *n*-octane [36], but for JP-10 it is one of the major product ions ($C_9H_{13}^+$).

For non-cyclic alkanes, the formation of many fragment ions is via the initial ionization at a σ bond between two carbons followed by the simple cleavage of the bond—the expulsion of an electron from the σ bond weakens the bond and brings about its direct dissociation [37]. For JP-10, with a multi-cyclic structure, multiple bond cleavages are required for the formation of any fragment ions. As seen in Fig. 3 and Table 1, $C_9H_{13}^+$ appears at electron energy of 11 eV, only 1.65 eV from the ionization energy of JP-10 (9.35 eV [38]). The cleavage of a C–H bond to eliminate an H atom in addition to cleavages of two C–C bonds to eliminate a CH_2 would have required more energy than 1.65 eV. An H rearrangement mechanism is therefore implied for the parent ion fragmentation forming $C_9H_{13}^+$. We propose an initial ionization site and σ bond cleavage to occur between C10 atom and C2 or C5 atom as labeled in Fig. 1, because the bond strain is the greatest at this site; the

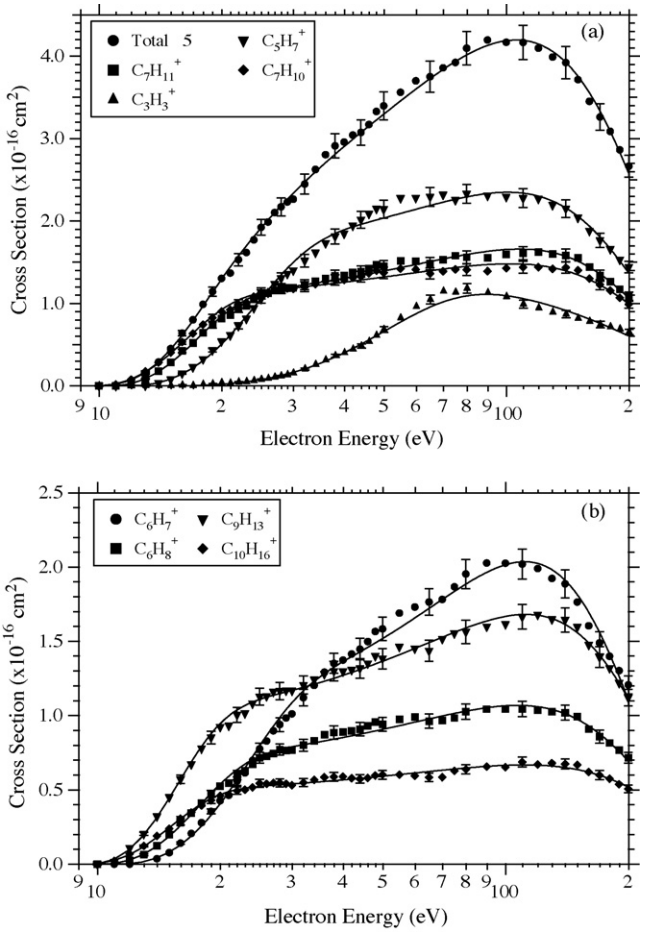

Fig. 3. Absolute total cross-section for electron ionization of JP-10 along with partial cross-sections for the 8 most abundant ions. The total cross-section is divided by 5 to allow display with the partial cross-sections. Symbols are measured data while solid curves are from a least-squares fit to an analytic function (see text). Error bars shown for selected data points are ± one standard deviation of the statistical error = ±5% of the cross-section value or 6×10^{-19}, whichever is larger. Estimated total uncertainty is ±18%.

cleavage of this bond results in a more stable ion than ions from other bond cleavages and therefore has a lower energy barrier.

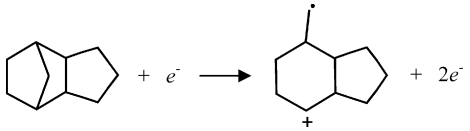

This parent ion undergoes γ-hydrogen rearrangement via a six-membered cyclic intermediate followed by subsequent loss of CH_3 to produce $C_9H_{13}^+$, which in turn yields $C_5H_7^+$ by eliminating a butadiene molecule through rearrangement of electron density:

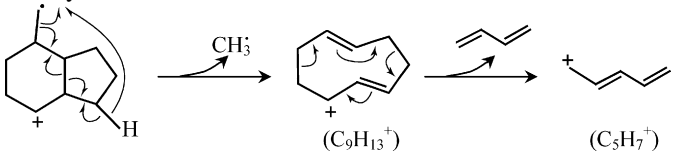

The driving force for this fragmentation is that the positive charges in the product ions are resonance-stabilized. Other important fragment ions can also be derived from the same parent ion structure:

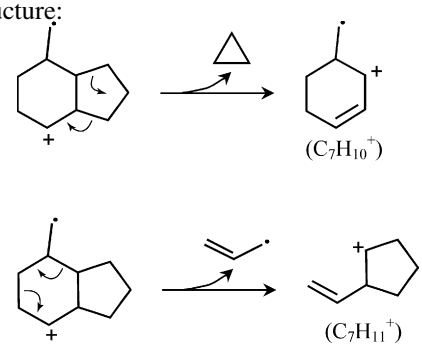

Secondary fragmentation of $C_7H_{10}^+$ produces $C_6H_8^+$ via radical-site induced hemolytic cleavage eliminating CH_2, and produces $C_6H_7^+$ via a four-center hydrogen migration and subsequent loss of CH_3, respectively:

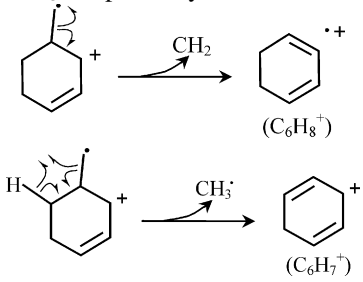

The parent–daughter relationship in the above primary and secondary fragmentation equations is in agreement with the order of the ion appearances as functions of the electron energy as seen in Fig. 3 or Table 1.

Solutions of the Boltzmann transport equation show that electron energy distribution functions (EEDF) in discharges in air–hydrocarbon mixtures are strongly nonequilibrium provided that the fractional ionization is not so high (>0.1%) that Coulomb collisions dominate the effects of electron-neutral collisions [39]. At low values of the normalized electric field, *E*/*N*, where *N* is the total gas density, over 80% of the fractional energy goes into vibrational excitation. This effect is caused by the large electron vibrational excitation cross-sections of nitrogen (a major component of air) in the range of 2–4 eV [40]. In a discharge, the resulting vibrational energy reservoir relaxes into translational energy or gas heating. When for ignition purposes, the discharge is pulsed with fast risetime (<1 μs) and overvolted, *E*/*N* attains high values, the electron mean energy correspondingly increases and more fractional energy goes into electronic excitation and ionization channels, including the dissociative ionization channels measured in this paper. To a good approximation in air:JP-10 mixtures, the ionization rates of the hydrocarbon molecules can be calculated using the 80% nitrogen:20% oxygen EEDF overlapped with the ionization cross-sections of this paper.

4. Summary

Electron impact ionization of the highly strained JP-10 molecule ($C_{10}H_{16}$) produces the parent ion and 36 fragment ions including $C_9H_{13}^+$, $C_5H_7^+$, $C_7H_{10}^+$, $C_7H_{11}^+$, $C_6H_8^+$, and $C_6H_7^+$, with an total cross-section peaking at 110 eV, of 2.19×10^{-15} cm^2. At electron energies below 27 eV, $C_9H_{13}^+$ is the predominant product ion, which is proposed to be formed

by an initial σ bond cleavage between C10 atom and C2 or C5 atom (see Fig. 1), followed by six-center γ-hydrogen rearrangement to eliminate CH_3 radical. Further fragmentation of $C_9H_{13}^+$ by rearrangement of electron density to eliminate a butadiene molecule is likely to be responsible for the formation of $C_5H_7^+$, which is the most abundant ion above 27 eV in the energy range studied.

Acknowledgements

The authors thank the Air Force Office of Scientific Research for support. We thank Dr. J.T. Edwards for providing the sample of JP-10.

References

[1] N.K. Smith, W.D. Good, AIAA J. 17 (1979) 905.
[2] J.E. Peters, A.M. Mellor, J. Energy 7 (1982) 95.
[3] G.A. Szekely Jr., G.M. Faeth, Combust. Flame 49 (1983) 255.
[4] R. Atkinson, S.M. Aschmann, W.P.L. Carter, Int. J. Chem. Kinet. 15 (1983) 37.
[5] P. Antaki, F.A. Williams, Combust. Flame 67 (1987) 1.
[6] L.C. Clausen, T.X. Li, C.K. Law, J. Propuls. Power 4 (1988) 217.
[7] S.C. Wong, S.R. Turns, Chem. Phys. Processes Combust. 97 (1988) 91.
[8] F. Takahashi, F.L. Dryer, F.A. Williams, Symp. (Int.) Combust. [Proc.] 21 (1988) 1983.
[9] F. Takahashi, I.J. Heilweil, F.L. Dryer, Combust. Sci. Technol. 65 (1989) 151.
[10] S.Y. Cho, F. Takahashi, F.L. Dryer, Combust. Sci. Technol. 67 (1989) 37.
[11] S.C. Wong, S.R. Turns, Combust. Sci. Technol. 66 (1989) 75.
[12] S.J. Guisinger, M.E. Rippen, Prepr.-Am. Chem. Soc., Div. Pet. Chem. 34 (1989) 885.
[13] S.C. Wong, A.C. Lin, Combust. Flame 89 (1992) 64.
[14] H.S. Chung, C.S.H. Chen, R.A. Kremer, J.R. Boulton, G.W. Burdette, Energy Fuels 13 (1999) 641.
[15] D.F. Davidson, D.C. Horning, J.T. Herbon, R.K. Hanson, Proc. Combust. Inst. 28 (2000) 1687.
[16] S.C. Li, B. Varatharajan, F.A. Williams, AIAA J. 39 (2001) 2351.
[17] J.M. Austin, J.E. Shepherd, Combust. Flame 132 (2003) 73.
[18] B. Varatharajan, M. Petrova, F.A. Williams, V. Tangirala, Proc. Combust. Inst. 30 (2005) 1869.
[19] S. Nakra, R.J. Green, S.L. Anderson, Combust. Flame 144 (2006) 662.
[20] P.N. Rao, D. Kunzru, J. Anal. Appl. Pyrolysis 76 (2006) 154.
[21] A. Osmont, I. Gokalp, L. Catoire, Prop. Explos. Pyrotech. 31 (2006) 343.
[22] B.V. Devener, S.L. Anderson, Energy Fuels 20 (2006) 1886.
[23] S.M. Starikovskaia, J. Phys. D: Appl. Phys. 39 (2006) R265.
[24] R. Maly, M. Vogel, Proceedings of the 17th Symposium (International) on Combustion, The Combustion Institute, Pittsburg, 1979, p. 821.
[25] S.M. Starikovskaia, N.B. Anikin, S.V. Pancheshnyi, D.V. Zatsepin, A.Y. Starikovskii, Plasma Sources Sci. Technol. 10 (2001) 344.
[26] C.Q. Jiao, C.A. DeJoseph Jr., A. Garscadden, J. Vac. Sci. Technol. A 23 (2005) 1295.
[27] M.B. Comisarow, A.G. Marshall, Chem. Phys. Lett. 25 (1974) 282.
[28] A.G. Marshall, P.B. Grosshans, Anal. Chem. 63 (1991) 215A.
[29] Z. Liang, A.G. Marshall, Anal. Chem. 62 (1990) 70.
[30] Kimball Physics, Inc., ELG-2A Electron Gun Instruction Manual, Kimball Physics, Inc., Wilton, New Hampshire, 1986.
[31] C.Q. Jiao, C.A. DeJoseph Jr., R. Lee, A. Garscadden, Int. J. Mass Spectrom. 257 (2006) 34.
[32] A.G. Marshall, T.L. Wang, T.L. Ricca, J. Am. Chem. Soc. 107 (1985) 7983.
[33] D.L. Rempel, S.K. Huang, M.L. Gross, Int. J. Mass Spectrom. Ion Processes 70 (1986) 163.
[34] H.C. Straub, P. Renault, B.G. Lindsay, K.A. Smith, R.F. Stebbings, Phys. Rev. A 52 (1995) 1115.
[35] C.Q. Jiao, C.A. DeJoseph Jr., A. Garscadden, J. Chem. Phys. 114 (2001) 2166.
[36] A. MacColl, Org. Mass Spectrom. 17 (1982) 1.
[37] E.D. Hoffmann, V. Stroobant, Mass Spectrometry, Principles and Applications, John Wiley & Sons, Ltd., Chichester, 2002.
[38] S.G. Lias, J.E. Bartmess, J.F. Liebman, J.L. Holmes, R.D. Levin, W.G. Mallard, J. Phys. Chem. Ref. Data 17 (1988).
[39] R. Nagpal, A. Garscadden, Contrib. Plasma Phys. 35 (1995) 301.
[40] G.J. Schulz, in: G. Bekefi (Ed.), Principles of Laser Plasmas, J. Wiley, New York, 1975.